



ORIGINAL ARTICLE

## Pathomorphological effects of Alloxan induced acute hypoglycaemia in rabbits

Masood Saleem Mir <sup>a,\*</sup>, Mohammad Maqbool Darzi <sup>a</sup>, Hilal Musadiq Khan <sup>b</sup>, Shayaib Ahmad Kamil <sup>a</sup>, Asif Hassan Sofi <sup>c</sup>, Sarfraz Ahmad Wani <sup>c</sup>

<sup>a</sup> Division of Veterinary Pathology, F.V.Sc. & A.H., Sher-e-Kashmir University of Agricultural Sciences and Technology of Kashmir, Shuhama, Alusteng, 190 006, Kashmir (J&K), India

<sup>b</sup> MRCSG, F.V.Sc. & A.H., Sher-e-Kashmir University of Agricultural Sciences and Technology of Kashmir, Shuhama, Alusteng, 190 006, Kashmir (J&K), India

<sup>c</sup> Division of LPT, F.V.Sc. & A.H., Sher-e-Kashmir University of Agricultural Sciences and Technology of Kashmir, Shuhama, Alusteng, 190 006, Kashmir (J&K), India

Received 16 January 2013; accepted 12 March 2013

Available online 9 April 2013

### KEYWORDS

Alloxan hypoglycaemia;  
Pathology;  
Rabbits

**Abstract** Alloxan is one of the frequently used beta-cytotoxic agents for the induction of Type-1 diabetes mellitus in animal models and is the drug of choice in rabbits. Its beta-cytotoxic action results in a sudden release of insulin leading to severe hypoglycaemia and even mortality if glucose therapy is not given. In the present investigation the pathological effects of alloxan induced acute hypoglycaemia were studied in rabbits. New Zealand White rabbits, 1–1.5 kg body weight, were administered alloxan @100 mg/kg b.w., as a single intravenous dose. Blood glucose levels were monitored (0 h, 20 min, 1 h, and then hourly up to 5 h) and clinical signs noted. Rabbits dead due to hypoglycaemia were necropsied and histopathology performed. Severe histopathological changes were observed especially in the brain (neuronal degeneration and necrosis), kidneys (nephrosis, nephritis) and liver (hepatosis, hepatitis) and also, other organs. Histopathological observation of beta-cytolysis was suggestive that the drug induced hypoglycaemia is insulin mediated. It was concluded that acute hypoglycaemia causes severe pathological changes and the alloxan induced immediate hypoglycaemia if not managed in time, might exacerbate the pathological effects of hyperglycaemia in the induced diabetic models.

© 2013 Production and hosting by Elsevier B.V. on behalf of Alexandria University Faculty of Medicine.

\* Corresponding author. Tel.: +91 946 9077920; fax: +91 194 2262536.

E-mail address: masoodmir1@gmail.com (M. Saleem Mir).

Peer review under responsibility of Alexandria University Faculty of Medicine.



Production and hosting by Elsevier

### 1. Introduction

Hypoglycaemia has been recognized as a medical exigency causing impaired brain function. The changes depend on the severity and duration of hypoglycaemia. Insulin induced hypoglycaemia has been one of the most important complications in the treatment of Type1 diabetes mellitus.<sup>1</sup> Hypoglycaemia can

trigger a sequence of events that may be extremely detrimental from the cardiac point of view. The increased mortality associated with the intensified insulin treatment arm of the Action to Control Cardiovascular Risk in Diabetes (ACCORD) trial has been ascribed to hypoglycaemia.<sup>2</sup> Studies have shown that hypoglycaemia induces proinflammatory changes.<sup>3–5</sup> Brain plays a dominant role in the activation of glucose counter regulatory defense systems. Measurements of glycogen levels in humans and rodents under different glycemic conditions have shown that acute hypoglycaemia depletes whole-brain glycogen stores in an attempt to maintain normal function. The brain glycogen stores begin to decline when brain glucose drops to near undetectable levels. However after hypoglycaemia, whole brain glycogen stores markedly increase above baseline levels, so-called supercompensation.<sup>1</sup> In addition to obvious short and long term effects of neuroglycopenia,<sup>6,7</sup> the brain is also vulnerable to systemic inflammation because cytokines from the circulation can potentially enter the brain, activate microglia and the neurotoxic sequence of events.<sup>8</sup>

Alloxan, a  $\beta$ -cytotoxic toxic glucose analogue,<sup>9</sup> is commonly used for the development of animal model of Type-I Diabetes Mellitus (IDDM).<sup>10</sup> Alloxan is rapidly taken up by the pancreatic  $\beta$ -cells through GLUT2 receptors.<sup>11</sup> Its beta-cytotoxic action results in sudden release of insulin leading to severe hypoglycaemia and even mortality if glucose therapy is not given. Rabbits are increasingly being used as experimental diabetic models and alloxan has been the chemical of choice for the development of rabbit models of diabetes.<sup>12–14</sup> The changes observed in these models are attributed to Alloxan induced diabetes, without any consideration of the effects of early hypoglycaemia. Present investigation was aimed at studying the pathological effects of alloxan induced acute hypoglycaemia in rabbits.

## 2. Materials and methods

New Zealand white rabbits three months of age and weighing about 1–1.5 kg were utilized in the study. The experimental protocols involved in this study were approved by the Institutional Animal Ethics Committee, Faculty of Veterinary Sciences and Animal Husbandry, SKUAST-K vide No. AU/FVS/Estt/C-09/7983-88 dated 19-01-2010 and conforms to the guidelines for the Care and Use of Laboratory Animals. All the animals were acclimatized for a period of 7 days prior to the commencement of the experiments. Rabbits were maintained under standard conditions in the cage system and offered feed and water *ad libitum*. Commercially procured rabbit feed and greens were given twice a day (morning and evening).

Alloxan monohydrate (Sigma–Aldrich) was administered to 18 rabbits, @100 mg/kg body weight in 1 ml sterile water as a single intravenous injection through the ear vein using an insulin syringe. Rabbits were fasted for 18 h prior to Alloxan administration and the dosage was selected on the basis of the available literature.

After the administration of beta-cytotoxic drugs, rabbits were monitored for changes in blood glucose levels using a glucometer (Accu-Chek, Roche diagnostics India Pvt. Ltd., Mumbai). Rabbits succumbing to hypoglycaemia were necropsied, gross lesions noted, and representative tissue samples from various organs were preserved in 10% buffered formal saline for histopathological examination. The tissues were processed by routine paraffin embedding technique and 5 $\mu$

sections stained with Harris Haematoxylin and Eosin. Parallel sections were stained with Alcian-Blue PAS (AB-PAS) for acid and neutral mucopolysaccharides. Pancreatic sections were also stained for the demonstration of pancreatic islet cells using Gomori's modified Aldehyde Fuchsin Stain.<sup>15</sup> Out of the 16 surviving rabbits, 11 developed hyperglycaemia on day 7 and were utilized as experimental diabetic models for further study. Five rabbits showed normal blood glucose levels range and were euthanized after 15 days.

## 3. Results

At 20 min post-administration of alloxan blood glucose levels declined from an average of  $112.83 \pm 3.270$  mg/dL to  $98.83 \pm 2.275$  mg/dL followed by an increasing trend up to 2 h ( $254.66 \pm 3.248$  mg/dL). Thereafter the blood glucose levels dropped progressively leading to severe hypoglycaemia by 5 h when glucose levels were between 30 and 58 mg/dL. Two rabbits showed convulsions and succumbed within 30 min after going into coma.

At necropsy, the rabbits revealed generalized congestion involving lungs, liver, kidneys, adrenals, pancreas and brain. Additionally the liver was darker, heart flabby and dilated, and the pancreas oedematous (Fig. 1).

Histopathologically, pancreas revealed loss of beta cells and degenerative changes in exocrine glands. Not all the islets were uniformly affected. Most of the islets had reduced cellularity with partial to complete loss of beta-cells. The mildly affected islets revealed beta-cell degranulation with increased cytoplasmic eosinophilia and loss of special staining character (Fig. 2). Some of the islets contained hyalinized cells where as at other places ghost islets with total loss of cells were also observed. Exocrine glands revealed degeneration and cytolysis. Blood vascular congestion was observed throughout the gland. Haemorrhages were present in the adnexa.

Brain revealed generalized vascular congestion and neuronal degeneration. Congestion of blood vessels in arachnoid and piamater, including choroid plexus, and cerebral microvasculature was consistently and widely observed (Fig. 3A). Focal areas of cerebral oedema were noted. Varying degrees of neuronal degeneration and necrosis, associated with gliosis and satellitosis, were noted in different cerebral cortical areas. Small pyramidal neurons in the second cortical layer appeared shrunken and stained darker with haematoxylin (Fig. 3B). Occasionally condensation and rounding of medium and large pyramidal cells in deeper layers were seen. Degeneration and necrosis of granule cells were evident in different strata of the cerebral cortex which was associated with demyelination. Inflammatory reaction was observed in the periependymal region. The cortical region adjacent to the periependymal area revealed degeneration of granule cells and dilation of the neuropil (Fig. 3C). Degeneration characterized by condensation of neurons, and dilation of neuropil associated with satellitosis was also observed in the caudoputamen. The hippocampus revealed neuronal degeneration and necrosis in all the regions. In the dentate gyrus, degeneration was more prominent in the granular cells at the crest, near the *cistern velum* but extended medially involving all the layers. Degenerative changes were characterized by neuronal condensation and dilation of the neuropil (Fig. 3D). Neuronal degeneration and necrosis associated with glial cell reaction and satellitosis were also,

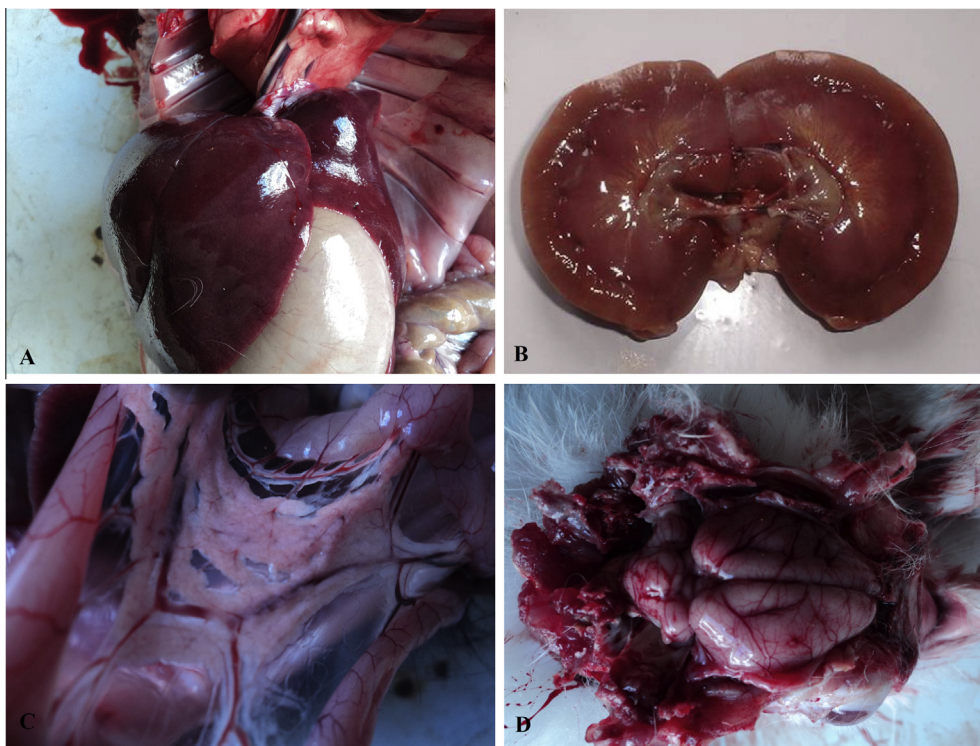


**Figure 1** Gross pathological changes in alloxan hypoglycaemic: (A) Liver appearing darker in colour and congested; (B) Kidneys revealing congestion of cortical and medullary regions; (C) Pancreas appearing soft, oedematous and congested; (D) Brain revealing vascular congestion.

observed in all the layers of *Cornu Ammonis*, CA1 region. Acidophilic necrosis and dilation of the neuropil were prominent in granule cells. The pyramidal cells in stratum pyramidale revealed increased basophilia, condensation and rounding of the soma. Neuronal degeneration, necrosis and dilation of neuropil were also, observed in granule cells of CA2 and CA3 regions but pyramidal cells in these regions were relatively less affected. The amygdaloid nuclei showed neuronal degeneration and necrosis with dilation of neuropil and gliosis. Areas closest to the lateral ventricles were more severely affected and at places revealed necrosis with accumulation of glial cells. Cerebellar meninges and vascular plexus were markedly congested. Severe microvascular congestion was observed in the cerebellar cortex including both the inner granular layer and the outer molecular layer. Haemorrhage was noted in the granular layer (Fig. 4A). Neuronal degeneration was evident in the granular and molecular layers, which was characterized by increased basophilia and condensation of the soma. Purkinje cells were not uniformly affected. While they were completely normal in some regions, degeneration and necrosis with the loss of cellular details as well as neuronolysis was observed in other areas (Fig. 4B). Staining of the parallel sections with combined Alcian Blue Periodic Acid Schiff (AB-PAS) technique revealed the nissl granules in normal pyramidal neurons and nucleus of the glial cells to be highly positive for acid mucopolysaccharides, while the cytoplasm of the pyramidal neurons was slightly positive (Fig. 4C). Degenerating and necrotic neurons including the degeneration of purkinje cells revealed loss of nissl substance and were only slightly positive for acid mucopolysaccharides (Fig. 4D). However, acid mucopolysaccharide reaction was normal in the granular layer.

Kidneys revealed vascular congestion and nephrotic changes both in cortical and medullary regions. Glomeruli were congested and frequently revealed hypercellularity and reduced peri-glomerular space (Fig. 5A). Some glomeruli revealed hypocellularity, hypersegmentation or shrinkage with the widening of peri-glomerular space. Convoluted tubules in the cortical region revealed degenerative changes characterized by swollen epithelium with indistinct cell boundaries and increased eosinophilia. Frequently necrosis and loss of tubular epithelium was noted. Focal nephritis associated with mononuclear cell infiltration was also observed (Fig. 5B). Vascular congestion was more prominent in the medullary region. Medullary tubules also revealed degeneration of the tubular epithelium characterized by cellular swelling and increased eosinophilia (Fig. 5C). Vacuolar changes were frequently observed. Focal interstitial nephritis was occasionally observed (Fig. 5D, E). AB-PAS staining revealed a nucleus of epithelial cells and the infiltrating cells, in the renal cortex and medulla, positive for acid mucopolysaccharides (Fig. 5F).

Liver revealed vascular congestion, hepatocellular degeneration, necrosis and sinusoidal dilatation. Hepatocellular necrosis was markedly characterized by nuclear pyknosis, karyorrhexis, karyolysis and indistinct cell boundaries (Fig. 6A). Severe vacuolar changes were observed especially in the sub-capsular region (Fig. 6B).

Lungs revealed wide-spread vascular engorgement and emphysema associated with atelectasis in adjacent areas (Fig. 7A). Mild degrees of haemorrhages were observed in the alveolar spaces. Peribronchial lymphoid hyperplasia was a frequent observation (Fig. 7B). AB-PAS staining revealed bronchial lining epithelium and peribronchial lymphoid tissue positive for acid mucopolysaccharides (Fig. 7C, D).

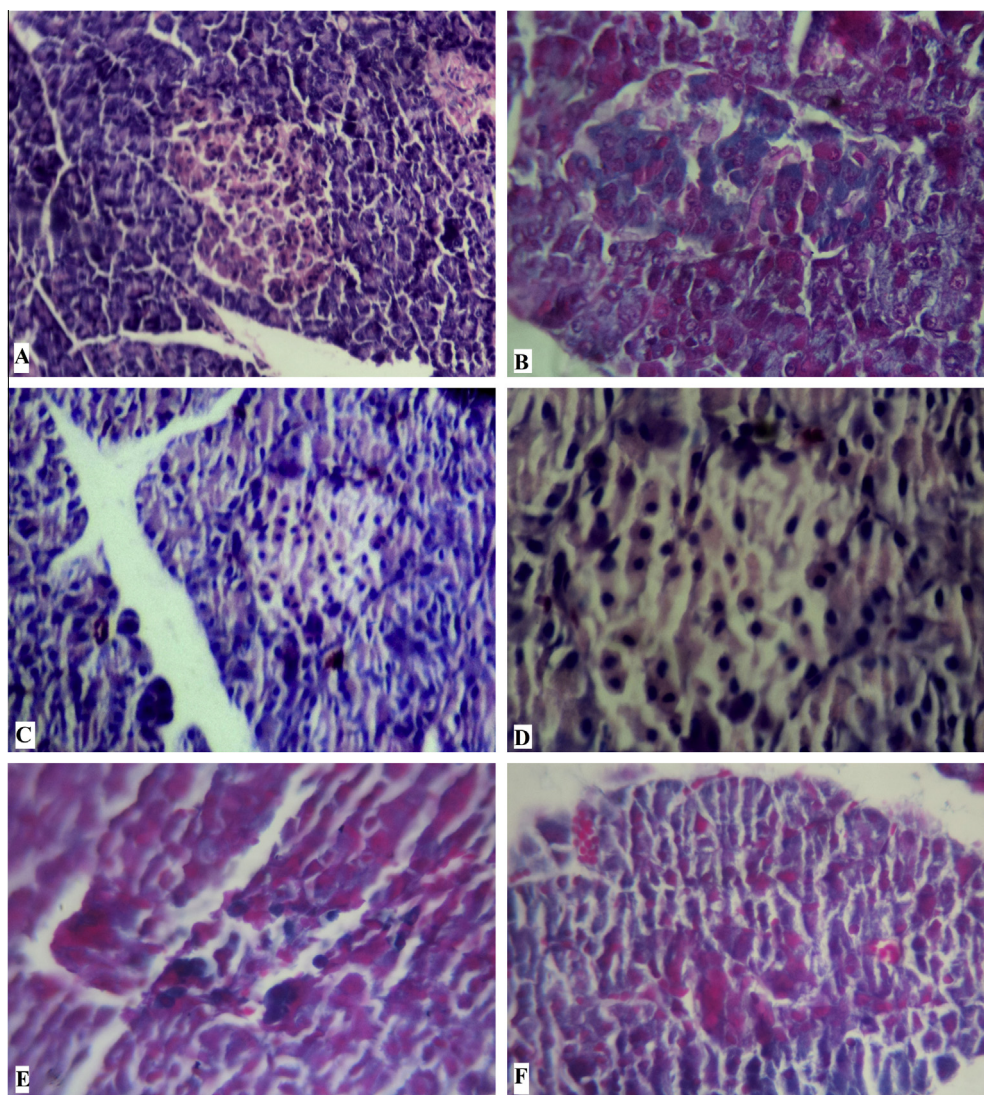


**Figure 2** Section of pancreas from control rabbit revealing (A) Normal islet and exocrine glands. H&E X100 (OZ x6.2), (B) Normal islet with beta-cells staining blue. MAF, X400 (OZ x3.5); and from alloxan hypoglycaemic rabbit revealing (C) Islet with reduced cellularity and acinar cell degeneration. H&E X100 (OZ x7.5), (D) Islet with reduced cellularity. H.E. X400 (OZ x4.1), (E, F) Islet with reduced cellularity due to beta-cell loss. MAF, X100 (OZ x3.5).

Heart revealed vascular congestion in epicardium, myocardium and endocardium (Fig. 8A). Myocytes revealed the cytoplasmic rarefaction with vacuolar appearance (Fig. 8B).

Vascular congestion and haemorrhages were prominent features in the spleen. Mild depletion of lymphoid cells was also observed focally (Fig. 9A).

Mesenteric lymph node (MLN) revealed lymphoid depletion causing thinning and rarefaction of the lymphoid tissue which was associated with a histiocytic reaction (Fig. 9B,C). Frequently congestion and haemorrhage were also observed (Fig. 9D).

Adrenal revealed mild haemorrhages in the cortex and degenerative changes in all the layers (Fig. 10A). Haemorrhage was more severe at the cortico-medullary junction (Fig. 10B).

#### 4. Discussion

The alloxan induced severe hypoglycaemia has been attributed to hyperinsulinaemia following beta-cytolysis caused by altered

redox potential and the generation of ROS<sup>16</sup> and disturbance in intracellular calcium homeostasis.<sup>17-19</sup> The  $\beta$ -cell degranulation and  $\beta$ -cytolysis was in consistency with pathomorphological alterations observed in the pancreas. Histopathologically, islets were variably affected ranging from degranulation to complete cytolysis. Species and individual variations in susceptibility to the beta-cytotoxic effects of Alloxan have been reported.<sup>20</sup> Present study confirms variation among islets from individual rabbit which may be attributed to a variation in the anti-oxidant status, besides the size and maturity of the cells. Also, the regeneration of  $\beta$ -cells, following Alloxan induced beta-cytolysis, has been recognized to start within 12 h.<sup>20,21</sup> The occasional presence of ghost islets reflect the susceptibility of non- $\beta$  islet cells to toxic effects of the drugs but need further investigation vis-à-vis their physiological status. Direct toxic effects of the drug on acinar cells have been reported by earlier workers.<sup>22</sup>

Alloxan induced hypoglycaemia was associated with marked and widespread CNS lesions. Besides vascular congestion,

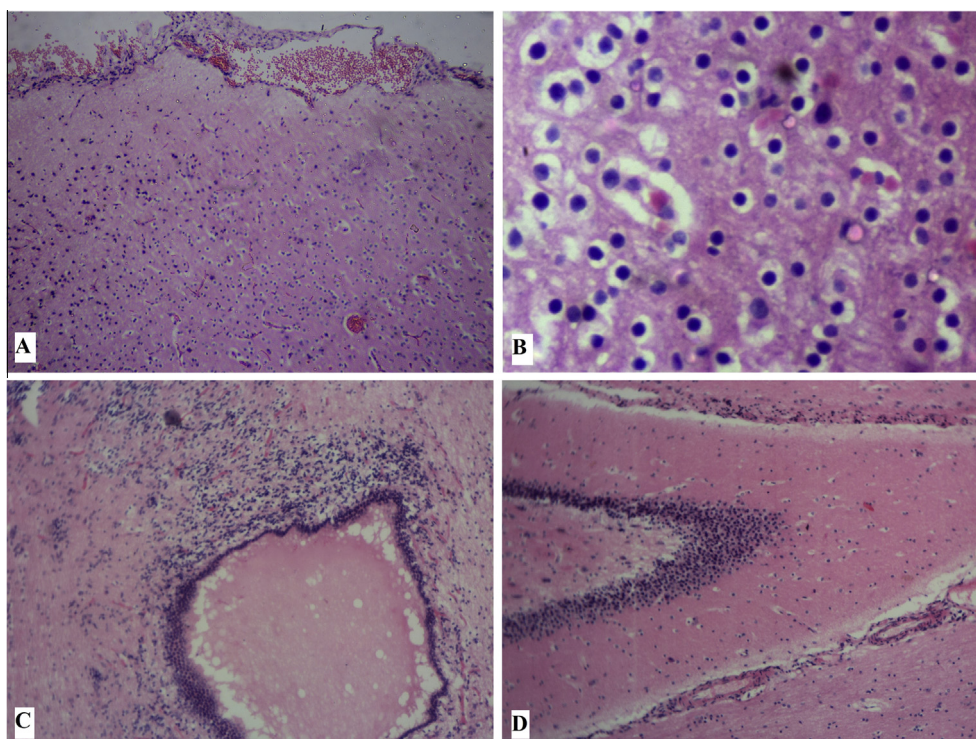


**Figure 3** Section of brain from alloxan hypoglycaemic rabbit revealing (A) Meningeal congestion. H&E X100 (OZ x3.0); (B) Shrinking of granule cells in cerebral cortex H&E X400 (OZ x3.5); (C) Inflammatory reaction in periependymal region. H&E X100 (OZ x4.0); (D) Degeneration of granule cells and dilation of neuropil in the dentate gyrus. H&E X100 (OZ x3.5).

degeneration of the choroid epithelium, and neuronal degeneration and necrosis were noted in all layers of the cerebral cortex, caudoputamen, different parts of the hippocampus including dentate gyrus, cornu ammonis, and subiculum as well as the cerebellum involving purkinje cells. The nature and pattern of histopathological changes observed are in concordance with the reports in the rat model.<sup>23</sup> Brain is especially sensitive to lowered blood glucose levels owing to limited glucose transport activity in the blood brain barrier and high rates of cellular glucose metabolism.<sup>24,25</sup> Dynamic measurement of glycogen levels, in humans and rodents under different glycaemic conditions, using *in vivo* nuclear magnetic resonance (NMR) spectroscopy has revealed the depletion of whole-brain glycogen stores following acute hypoglycaemia in an attempt to maintain normal function.<sup>26–28</sup> Certain areas like layer 2 of the cerebral cortex, and subiculum and dentate gyrus in the hippocampus, especially those closest to the ventricles were more severely and consistently affected. This is in agreement with the earlier reports of regional variation in the susceptibility of brain to hypoglycaemia induced injury.<sup>1,29</sup> An endogenous excitotoxin (neurotoxin) has been ascribed for the observed effects.<sup>30–32</sup> It has been observed that at glucose levels below 1 mM (18 mg/dL), there is abrupt brain energy failure causing flat EEG and results in massive release of the excitatory amino acid aspartate leading to neuronal calcium fluxes and necrosis. The accumulation of this toxin in CSF has been incriminated for observed special differences in the affection of homogenous neuronal populations. Other neurochemical changes include energy depletion, phospholipase and other enzyme activation, tissue alkalosis and a tendency for all cellular redox systems to shift towards oxidation.<sup>29</sup> Condensation and increased basophilia was a characteristic feature

of neuronal necrosis. Acidophilic necrosis was occasionally observed. This, also, supports a prominent role of the neurotoxin, rather than tissue alkalosis, in neuronal necrosis. However, role of reduced regional blood flow in association with hypoglycaemia<sup>33</sup> needs to be evaluated.

Further, in present study, changes were also observed in the white matter. Although, majority of studies report involvement of only grey matter, case studies in human have shown extensive white matter injuries either alone or in association with lesions in grey matter.<sup>34,35</sup> Studies have shown that glycogen plays an important role in protecting white matter against this injury.<sup>36</sup> Only astrocytes (not neurons or oligodendrocytes) contain glycogen which is utilized during hypoglycaemia and staves off injury. The period of protection from hypoglycaemic injury is determined by astrocyte glycogen content.<sup>37</sup>

In the present study, lesions were also noted in the cerebellum involving purkinje cells, and the spinal cord. This is contrary to earlier reports wherein the cerebellum has been invariably reported to be resistant to hypoglycaemia,<sup>29</sup> and may be ascribed to either the more severe nature of hypoglycaemia in the present study or to a fall in blood flow.<sup>33</sup> Kim and coworkers<sup>38</sup> also reported an unusual case of episodic bilateral cerebellar dysfunction caused by hypoglycaemia, with a quantitative dynamic PET study demonstrating decreased glucose uptake-to-utilization ratio and increased leak of glucose in the cerebellum. They suggested that the cerebellum is not invariably resistant to hypoglycaemia.

Renal lesions observed in Alloxan, and Alloxan-STZ hypoglycaemia were characterized by vascular congestion, tubular nephrosis and necrosis involving convoluted tubules and lower

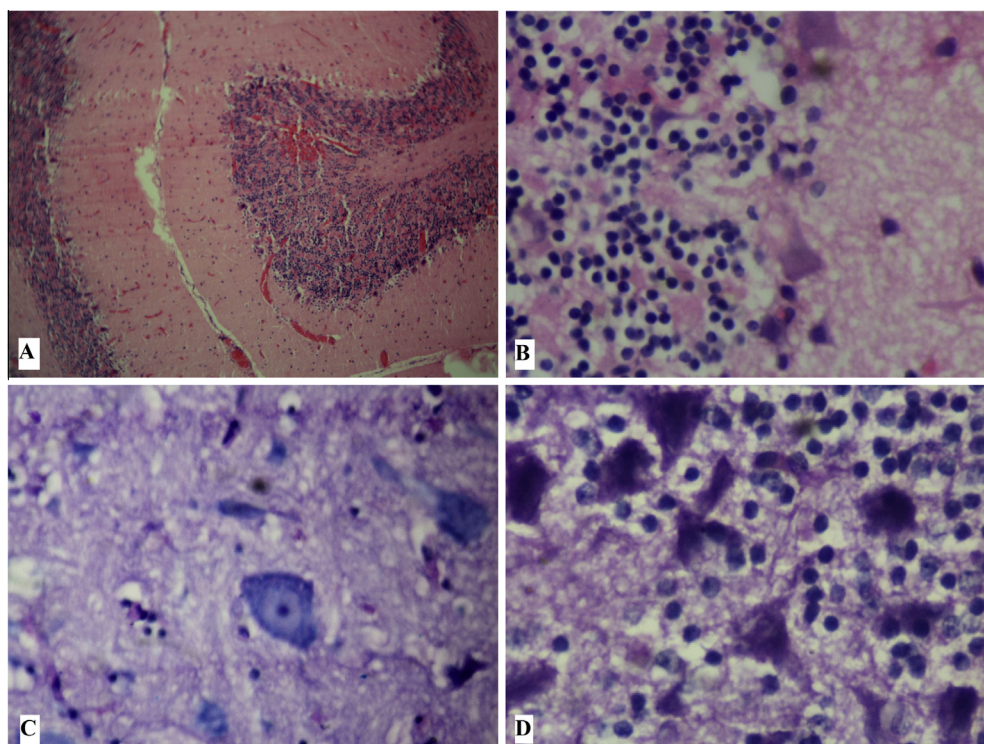


**Figure 4** Section of brain from alloxan hypoglycaemic rabbit revealing (A) Severe vascular congestion and haemorrhage of cerebellum H.E. X100 (OZ x3.0); (B) Degeneration of purkinje cells in the cerebellum. H.E. X400 (OZ x3.3); (C) The Nissl granules in normal pyramidal neurons and nucleus of the glial cells are highly positive, while the cytoplasm of the pyramidal neurons is slightly positive for acid mucopolysaccharides. AB-PAS, x400 (OZ x2.8), (D) Glial cells are more positive for acid mucopolysaccharides than degenerating neurons. AB-PAS, x400 (OZ x4.3).

nephron, glomerular congestion and hypercellularity with reduced Bowman's space, and interstitial nephritis. Renal tubular epithelium expresses high levels of Glut2 glucose transporter,<sup>39</sup> and hence is sensitive to both Alloxan and STZ toxicities although it is partially protected by higher antioxidant status. Direct nephrotoxic effects of Alloxan have been demonstrated.<sup>40</sup> Further, kidneys play an essential role in glycaemic control and respond promptly to changes in blood glucose levels.<sup>41,42</sup> Hyperinsulinemic-hypoglycaemic state has been observed to shift renal glucose balance towards net release as a part of counterregulatory mechanism.<sup>43,44</sup> The condition if prolonged may lead to an energy crisis resulting in renal damage. Patrick and coworkers<sup>45</sup> reported that acute insulin-induced hypoglycaemia resulted in decreased renal blood flow, decreased excretion of sodium and dopamine, whereas albumin excretion was unaltered. However, contrary to this several experimental and clinical studies have shown that insulin resistance and hyperinsulinemia induced renal vasodilation causing glomerular hypertension and hyperfiltration, which may predispose individuals to progressive renal dysfunction.<sup>46-48</sup> In conditions of acute hyperinsulinemia, by the administration of exogenous insulin in normal rats, renal plasma flow and the glomerular hydrostatic pressure gradient increased significantly because of more dilation of afferent arterioles than efferent ones.<sup>46</sup> Hyperinsulinaemia has been reported to promote the proliferation of renal cells, and stimulate the production of insulin-like growth factor-1 and transforming growth factor- $\beta$ . It also upregulates the expression of angiotensin-II type 1 receptor in mesangial cells, thus enhancing the deleteri-

ous effects of angiotensin-II in the kidney, and stimulates the production and renal action of endothelin-1.<sup>49</sup>

Liver lesions in Alloxan-induced hypoglycaemia included congestion, hepatosis and necrosis. Alloxan-STZ induced hypoglycaemia additionally revealed hepatitis and Kupffer cell hyperplasia. Acute hepatopathy, like nephropathy, may be ascribed to direct drug-induced toxicity, hypoglycaemia, or hyperinsulinaemia. Glut2 has been found to be expressed at a very high level in the basolateral membranes of hepatocytes<sup>39</sup> making them subjects for direct toxicity. Alloxan induced time- and concentration-dependent damage has been evidenced.<sup>50</sup> At concentrations of 3.5 mM and above, Alloxan caused an increase in lactate dehydrogenase (LDH), glutamate-pyruvate transaminase (GPT) and intracellular potassium ( $K^+$ ) leakage, all of which are indices of plasma membrane damage, and decreased the intracellular reduced glutathione content (GSH) in suspensions of isolated rat hepatocytes which were partially protected by Preincubation (10 min) in D-glucose (50 or 100 mM, but not 10 mM).<sup>51</sup> Hyperinsulinaemic hypoglycaemia has been reported to alter liver function in the cow.<sup>52</sup>

Observation of only mild changes in cardiac muscles may be attributed to the fact that it uses fatty acid oxidation as the main source of energy while glucose and lactate account for only ~30% of energy.<sup>53</sup> Further, heart can rapidly switch its substrate selection to accommodate different physiological and pathophysiological conditions.<sup>54,55</sup>

The generalized vascular congestion was a consistent feature. This may be attributed to hypoglycaemia induced

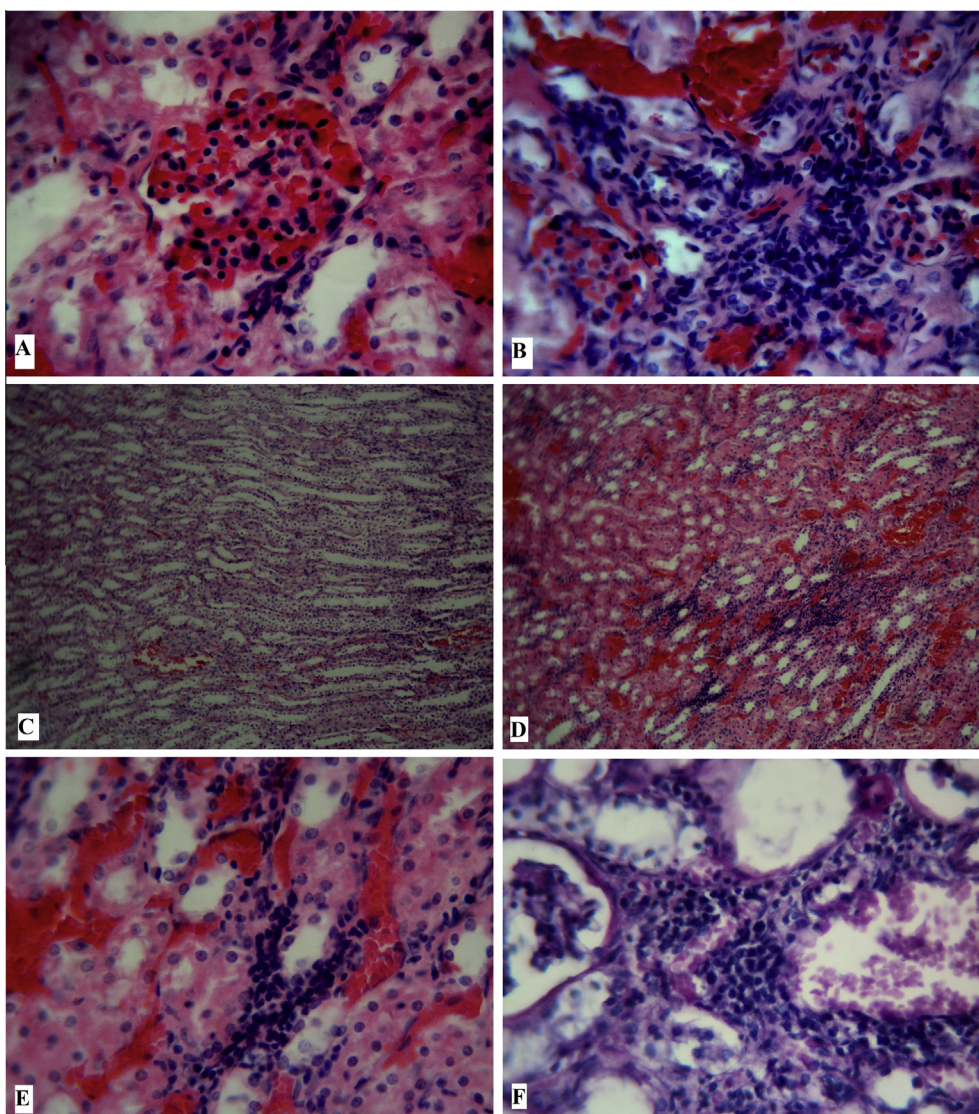


**Figure 5** Section of kidney from alloxan hypoglycaemic rabbit revealing (A) Glomerular congestion, mesangial hyperplasia and degeneration of the lining epithelium of PCTs (H&E X400) (OZ x4.0); (B) Focal interstitial nephritis and glomerular and vascular congestion. H&E X400 (OZ x4.0); (C) Vascular congestion, and lower nephron nephrosis. H&E X100 (OZ x3.0); (D) Vascular congestion, haemorrhage, lower nephron nephrosis and focal nephritis. H&E X100 (OZ x3.0); (E) Vascular congestion, lower nephron nephrosis and focal nephritis. H&E X400 (OZ x3.5); (F) Infiltrating cells in the renal cortex staining positive for acid-mucopolysaccharide. AB-PAS, X400 (OZ x4.0).

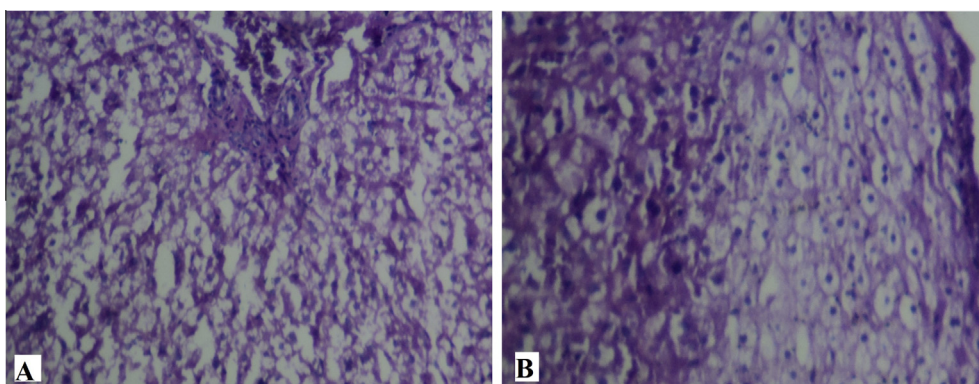


**Figure 6** Section of the liver from alloxan hypoglycaemic rabbit revealing (A) Severe degeneration of hepatocytes. AB-PAS, X100 (OZ x5.7); (B) Severe vacuolar changes in the subcapsular region. AB-PAS, X100 (OZ x8.3).

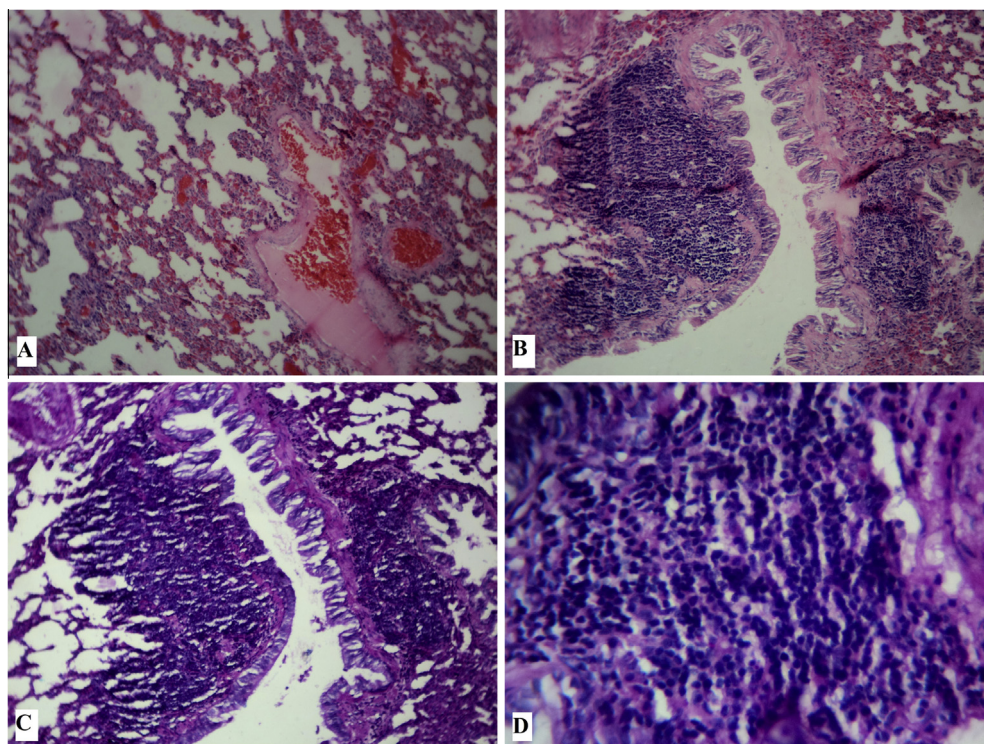


**Figure 7** Section of lungs revealing (A) Vascular engorgement, emphysema and atelectasis. H&E X100 (OZ x3.0); (B) Peribronchial lymphoid hyperplasia. H&E X100 (OZ x3.0); (C) Peribronchial lymphoid tissue and bronchial epithelium positive for acid mucopolysaccharides. AB-PAS, X100 (OZ X3.0); (D) Acid mucopolysaccharides positive peribronchial lymphoid tissue. AB-PAS, X400 (OZ x4.0).

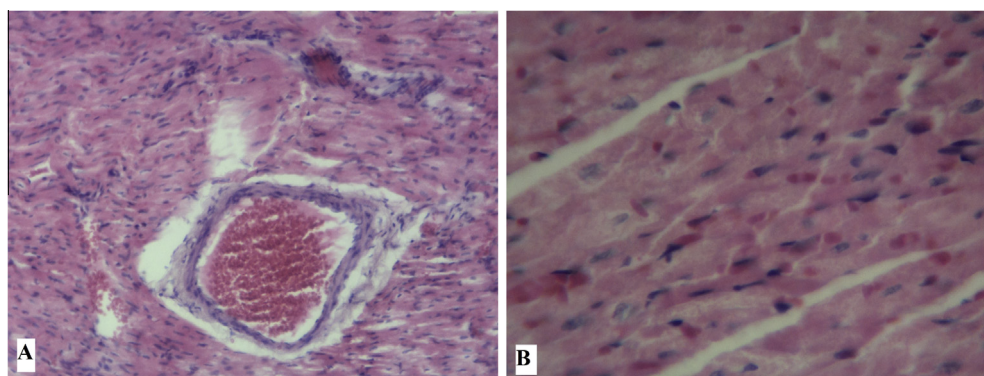


**Figure 8** Alloxan hypoglycaemic rabbit, section of heart revealing (A) Vascular congestion. H&E X100 (OZ x6.0); (B) Micro-vascular congestion and cytoplasmic rarefaction with vacuolar appearance. H.E. X400 (OZ x5.5).

increase in blood flow and decreased vascular resistance.<sup>56</sup> Inflammatory response was a consistent feature in different organs viz. interstitial nephritis, Kupffer cell hyperplasia and hepatitis, peribronchial lymphoid hyperplasia, and histiocytic reaction in MLNs. This may be attributed primarily to acute inflammatory response to hyperinsulinaemia which might be further augmented by tissue damage. Short-term exposure to hyperinsulinaemia has been shown to upregulate a number of genes involved in inflammation viz. thrombomodulin, inflammatory chemokines (CCL8, CXCL2, and CCL2) and cytokines (interleukin-1 receptor type I and interferon- $\gamma$ -inducible protein-16).<sup>57-59</sup> These results are consistent with the

histopathological observation that the inflammatory cells were principally mononuclear cells. The mild depletion of lymphoid cells in the spleen and MLN may be attributed to their mobilization under the influence of an acute release of chemotactic factors. Further, the generalized vascular disturbance including congestion and haemorrhages were observed in all the organs. Upregulation and release of vasoactive substances has been suggested as a putative mechanism for hypoglycaemic vascular injury.<sup>4</sup> Hypoglycaemia has been incriminated as one of the important factors for pulmonary hypertension in human neonates.<sup>60</sup> A similar mechanism may be responsible for the observed lung congestion, oedema and emphysema.



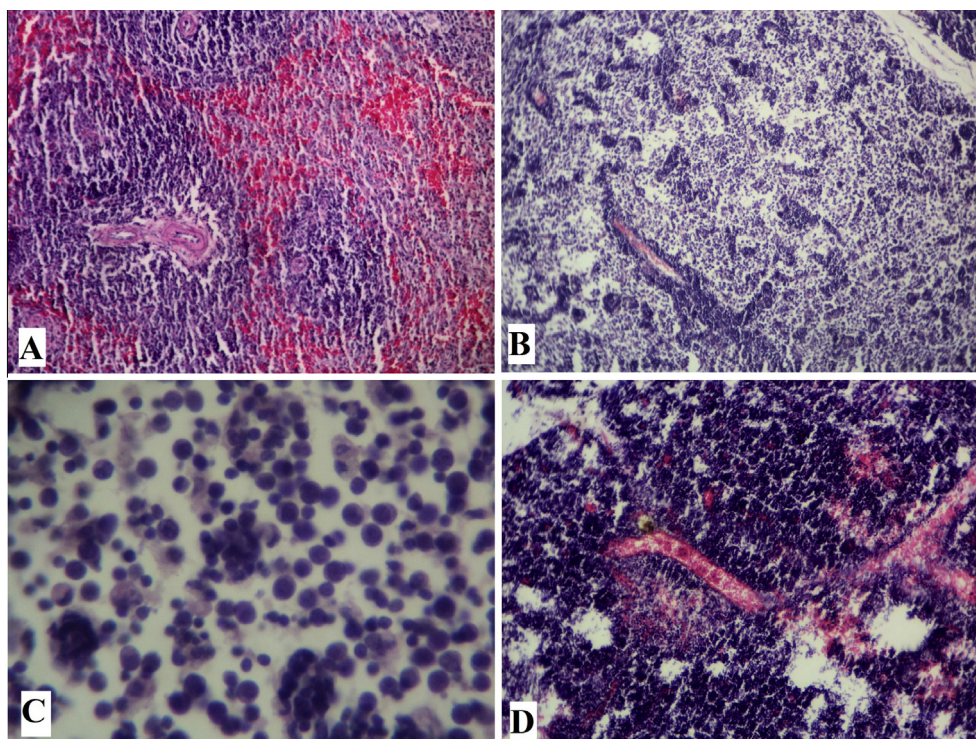


**Figure 9** Section of spleen revealing (A) Mild depletion of lymphocytes and haemorrhage. H&E X100 (OZ x3.5); Section of mesenteric lymph node showing (B) Lymphoid depletion with histiocyte reaction. H&E X100 (OZ x3.0); (C) Higher magnification of d. H&E X400 (OZ x6.2); (D) Lymphoid depletion, congestion and haemorrhage. H&E X100 (OZ x3.5).

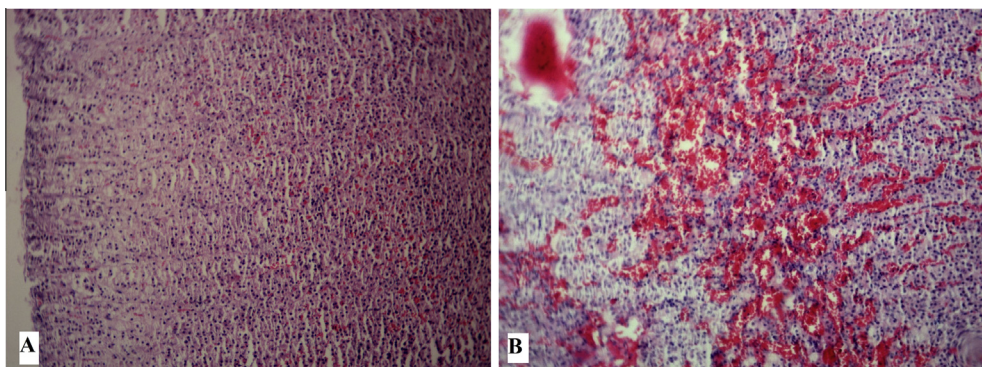


**Figure 10** Alloxan hypoglycaemic rabbit Section of the adrenal gland revealing (A) Mild haemorrhage in the cortex, and degenerative changes in zona glomerulosa and zona fasciculata. H&E X100 (OZ x3.0); (B) Congestion and haemorrhage in the cortex and medulla. H.E. X100 (OZ x2.8).

## 5. Conclusion

It is concluded that Alloxan induced acute-hypoglycaemia caused severe pathological alterations especially in vital organs viz. brain, kidneys and liver. The changes may be attributed partly to direct toxic effects of the chemicals, and partly to drug induced hyperinsulinaemia and hypoglycaemia. If not managed in time, hypoglycaemia might exacerbate the hyperglycaemia-induced pathological effects in the induced diabetic models.

## References

1. Herzog RI, Chan O, Yu S, Dziura J, McNay EC, Sherwin RS. Effect of acute and recurrent hypoglycemia on changes in brain glycogen concentration. *Endocrinology* 2008;**149**(4):1499–504.
2. Dandona P, Chaudhuri A, Dhindsa S. Proinflammatory and prothrombotic effects of Hypoglycemia. *Diabetes Care* 2010;**33**(7):1686–7.
3. Razavi-Nematollahi L, Kitabchi AE, Kitabchi AE, Stentz FB, Wan JY, Larijani BA, et al. Proinflammatory cytokines in

- response to insulin-induced hypoglycemic stress in healthy subjects. *Metabolism* 2009;**58**:443–8.
4. Wright RJ, Newby DE, Stirling D, Ludlam CA, Macdonald IA, Frier BM. Effects of acute insulin-induced hypoglycemia on indices of inflammation putative mechanism for aggravating vascular disease in diabetes. *Diabetes Care* 2010;**33**(7):1591–7.
  5. Gogitidze-Joy N, Hedrington MS, Briscoe VJ, Tate DB, Ertl AC, Davis SN. Effects of acute hypoglycemia on inflammatory and pro-atherothrombotic biomarkers in individuals with type 1 diabetes and healthy individuals. *Diabetes Care* 2010;**33**:1529–35.
  6. Guettier JM, Gorden P. Hypoglycemia. *Endocrinol Metabol Clin North Am* 2006;**35**:753–66.
  7. Lin YY, Hsu CW, Sheu WHH, Chu SJ, Wu CP, Tsai SH. Risk factors for recurrent hypoglycemia in hospitalized diabetic patients admitted for severe hypoglycaemia. *Yonsei Med J* 2010;**51**(3):367–74.
  8. Van-Gool WA, van de Beek D, Eikelenboom P. Systemic infection and delirium: when cytokines and acetylcholine collide. *Lancet* 2010;**375**:773–5.
  9. Gorus FK, Malaisse WJ, Pipeleers DG. Selective uptake of alloxan by pancreatic B-cells. *Biochem J* 1982;**208**:513–5.
  10. Szkudelski T. The mechanism of alloxan and streptozotocin action in  $\beta$ -cells of the rat pancreas. *Physiol Res* 2001;**50**:536–46.
  11. Elsner M, Tiedge M, Guldbakke B, Munday R, Lenzen S. Importance of the GLUT2 glucose transporter for pancreatic beta cell toxicity of alloxan. *Diabetologia* 2002;**45**:1542–9.
  12. Sharma SB, Nasir A, Prabhu KM, Murthy PS, Dev G. Hypoglycaemic and hypolipidemic effect of ethanolic extract of seeds of *Eugenia jambolana* in alloxan-induced diabetic rabbits. *J Ethnopharmacol* 2003;**85**:201–6.
  13. Gupta RK, Kesari AN, Watal G, Murthy PS, Chandra R, Tandon V. Nutritional and hypoglycemic effect of fruit pulp of *Annona squamosa* in normal healthy and alloxan-induced diabetic rabbits. *Annals Nut Metabol* 2005;**49**:407–13.
  14. El-Said EE, El-Sayed GR, Tantawy E. Effect of camel milk on oxidative stress in experimentally induced diabetic rabbits. *Vet Res Forum* 2010;**1**(1):30–43.
  15. Luna LG. *Manual of histologic staining methods of the armed forces institute of pathology*. 3rd ed. New York: McGraw-Hill Book Company; 1968.
  16. Elsner M, Gurgul-Convey E, Lenzen S. Relative importance of cellular uptake and reactive oxygen species for the toxicity of alloxan and dialuric acid to insulin-producing cells. *Free Rad Biol Med* 2006;**41**:825–34.
  17. Weaver DC, McDaniel ML, Naber SP, Barry CD, Lacy PE. Alloxan stimulation and inhibition of insulin release from isolated rat islets of Langerhans. *Diabetes* 1978;**27**:1205–14.
  18. Kim HR, Rho HW, Park JW, Kim JS, Kim UH, Chung MY. Role of  $Ca^{2+}$  in alloxan-induced pancreatic beta-cell damage. *Biochim Biophys Acta* 1994;**1227**:87–91.
  19. Park BH, Rho HW, Park JW, Cho CG, Kim JS, Chung HT, et al. Protective mechanism of glucose against alloxan-induced pancreatic beta-cell damage. *Biochem Biophys Res Commun* 1995;**210**:1–6.
  20. Tyrberg B, Andersson A, Borg LA. Species differences in susceptibility of transplanted and cultured pancreatic islets to the beta-cell toxin alloxan. *Gen Compar Endocrinol* 2001;**122**(3):238–51.
  21. Nagasao J, Yoshioka K, Amasaki H, Tsujio M, Ogawa M, Taniguchi K, et al. Morphological changes in the rat endocrine pancreas within 12 h of intravenous streptozotocin administration. *Anatom Histol Embryol* 2005;**34**(1):42–7.
  22. Sano T, Ozaki K, Matsuura T, Narama I. Giant mitochondria in pancreatic acinar cells of alloxan-induced diabetic rats. *Toxicol Pathol* 2010;**38**:658–65.
  23. Auer RN, Wieloch T, Olsson Y, Siesj BK. The distribution of hypoglycemic brain damage. *Acta Neuropathol (Berlin)* 1984;**64**:177–91.
  24. Abi-Saab WM, Maggs DG, Jones T, Jacob R, Srihari V, Thompson J, et al. Striking differences in glucose and lactate levels between brain extracellular fluid and plasma in conscious subjects with epilepsy: effects of hyperglycemia and hypoglycemia. *J Cerebral Bl Flow Metabol* 2002;**22**:271–9.
  25. Sherwin RS. Bringing light to the dark side of insulin: a journey across the blood–brain barrier. *Diabetes* 2008;**57**(9):2259–68.
  26. Choi IY, Tkac I, Ugurbil K, Gruetter R. Noninvasive measurements of  $1\text{-}^{13}\text{C}$  glycogen concentrations and metabolism in rat brain in vivo. *J Neurochem* 1999;**73**:1300–8.
  27. Choi IY, Seaquist ER, Gruetter R. Effect of hypoglycemia on brain glycogen metabolism in vivo. *J Neurosci Res* 2003;**72**:25–32.
  28. Oz G, Henry PG, Seaquist ER, Gruetter R. Direct, noninvasive measurement of brain glycogen metabolism in humans. *Neurochem Int* 2003;**43**:323–9.
  29. Auer RN. Hypoglycemic brain damage. *For Sci Int* 2004;**146**(2):105–10.
  30. Wieloch T. Hypoglycemia-induced neuronal damage prevented by an N-methyl-D-aspartate antagonist. *Science* 1985;**230**:681–3.
  31. Wieloch T, Engelsen B, Westerberg E, Auer R. Lesions of the glutamatergic cortico-striatal projections ameliorate hypoglycemic brain damage in the striatum. *Neurosci Lett* 1985;**58**:25–30.
  32. Lindvall O, Auer RN, Siesj BK. Selective lesions of mesostriatal dopamine neurons ameliorate hypoglycemic damage in the caudate-putamen. *Exp Brain Res* 1986;**63**(2):382–6.
  33. Teves D, Videen TO, Cryer PE, Powers WJ. Activation of human medial prefrontal cortex during autonomic responses to hypoglycaemia. *Proc Natl Acad Sci* 2004;**101**(16):6217–21.
  34. Mori F, Nishie M, Houzen H, Yamaguchi J, Wakabayashi K. Hypoglycemic encephalopathy with extensive lesions in the cerebral white matter. *Neuropathology* 2006;**26**(2):147–52.
  35. Kim JH, Koh SB. Extensive white matter injury in hypoglycemic coma. *Neurology* 2007;**68**:1074.
  36. Wender R, Brown AM, Fern R, Swanson RA, Farrell K, Ransom BR. Astrocytic glycogen influences axon function and survival during glucose deprivation in central white matter. *J Neurosci* 2000;**20**:6804–10.
  37. Goldberg MP, Ransom BR. New Light on White Matter. *Stroke* 2003;**34**:330–2.
  38. Kim DE, Park SH, Kim SK, Nam HW, Lee YS, Chung JK, et al. Hypoglycemia-induced cerebellar dysfunction and quantitative positron emission tomography study. *Neurology* 2000;**55**(3):418–22.
  39. Uldry M, Thorens B. The SLC2 family of facilitated hexose and polyol transporters. *Pflugers Archiv* 2004;**447**(5):480–9.
  40. Evan AP, Mong SA, Connors BA, George R, Aronoff GR, Luft FC. The effect of alloxan, and alloxan-induced diabetes on the kidney. *Anatom Rec* 1984;**208**(1):33–47.
  41. Adroque HJ, Comstock JP, Pena J, Hartley C, Entman M, Rashad MN. Large renal glucose production (RGP) in conscious diabetic dogs without acidosis. *Diabetes* 1990;**39**:24A.
  42. Cersosimo E, Judd RL, Miles JM. Insulin regulation of renal glucose metabolism in conscious dogs. *Journal Clin Invest* 1994;**93**:2584–9.
  43. Meyer C, Dostou JM, Gerich JE. Role of the human kidney in glucose counterregulation. *Diabetes* 1999;**48**:943–8.
  44. Cersosimo E, Garlick P, Ferretti J. Renal glucose production during insulin-induced hypoglycemia in humans. *Diabetes* 1999;**48**(2):261–6.
  45. Patrick AW, Hepburn DA, Craig KJ, Thomson I, Swainson CP, Frier BM. The effects of acute insulin-induced hypoglycaemia on renal function in normal human subjects. *Diabetic Med* 1989;**6**(8):703–8.
  46. Tucker BJ, Anderson CM, Thies RC, Collins RC, Blantz RC. Glomerular hemodynamic alterations during acute hyperinsulinemia in normal and diabetic rats. *Kidney Int* 1992;**42**:1160–8.
  47. Dengel DR, Goldberg AP, Mayuga RS, Kairis GM, Weir MR. Insulin resistance, elevated glomerular filtration fraction, and renal injury. *Hypertension* 1996;**28**:127–32.
  48. Kubo M, Kiyohara Y, Kato I, Iwamoto H, Nakayama K, Hirakata H, et al. Effect of hyperinsulinemia on renal function in

- a general Japanese population: the Hisayama study. *Kidney Int* 1999;**55**:2450–6.
49. Sarafidis PA, Ruilope LM. Insulin resistance, hyperinsulinemia, and renal injury: mechanisms and implications. *Am J Nephrol* 2006;**26**:232–44.
  50. Fan W, Liu A, Wang W, Zheng G, Teng A. Hepatoprotective activity of CrPic against alloxan-induced hepatotoxicity in mice. *Biol Trace Element Res* 2012;**149**(2):227–33.
  51. Harman AW, Fischer LJ. Alloxan toxicity in isolated rat hepatocytes and protection by sugars. *Biochem Pharmacol* 1982;**31**(23):3731–6.
  52. Kreipe L, Vernay MCMB, Oppliger A, Wellnitz O, Bruckmaier HA, van Dorland HA. Induced hypoglycemia for 48 hours indicates differential glucose and insulin effects on liver metabolism in dairy cows. *J Dairy Sci* 2011;**94**(11):5435–48.
  53. Saddik M, Lopaschuk GD. Myocardial triglyceride turnover and contribution to energy substrate utilization in isolated working rat hearts. *J Biol Chem* 1991;**266**:8162–70.
  54. Atkinson LL, Fischer MA, Lopaschuk GD. Leptin activates cardiac fatty acid oxidation independent of changes in the AMP-activated protein kinase-acetyl-CoA carboxylase-malonyl-CoA axis. *J Biol Chem* 2002;**277**:29424–30.
  55. Koonen DP, Glatz JF, Bonen A, Luiken JJ. Long-chain fatty acid uptake and FAT/CD36 translocation in heart and skeletal muscle. *Biochim Biophys Acta* 2005;**1736**:163–80.
  56. Hoffman RP, Sinkey CA, Tsalikian E. Effect of local sympathetic blockade on forearm blood flow and glucose uptake during hypoglycemia. *Metabolism* 1999;**48**:1575–83.
  57. Rome S, Clement K, Rabasa-Lhoret R, Loizon E, Poitou C, Barsh GS, et al. Microarray profiling of human skeletal muscle reveals that insulin regulates approximately 800 genes during a hyperinsulinemic clamp. *J Biol Chem* 2003;**278**:18063–8.
  58. Hansen L, Gaster M, Oakeley EJ, Brusgaard K, Damsgaard Nielsen EM, Beck-Nielsen H, et al. Expression profiling of insulin action in human myotubes: induction of inflammatory and pro-angiogenic pathways in relationship with glycogen synthesis and type 2 diabetes. *Biochem Biophys Res Commun* 2004;**323**:685–95.
  59. Coletta DK, Balas B, Chavez AO, Baig M, Abdul-Ghani M, Kashyap SR, et al. Effect of acute physiological hyperinsulinemia on gene expression in human skeletal muscle in vivo. *Am J Physiol – Endocrinol Metabol* 2008;**294**(5), E910-E917.
  60. Dakshinamurti S. Pathophysiologic mechanisms of persistent pulmonary hypertension of the newborn. *Pediatric Pulmonol* 2005;**39**(6):492–503.